



**HAL**  
open science

## Quasi-1D Polymer Semiconductor–Diarylethene Blends: High Performance Optically Switchable Transistors

Yusheng Chen, Hanlin Wang, Hu Chen, Weimin Zhang, Shunqi Xu, Michael Pätzelt, Chun Ma, Cang Wang, Iain Mcculloch, Stefan Hecht, et al.

► **To cite this version:**

Yusheng Chen, Hanlin Wang, Hu Chen, Weimin Zhang, Shunqi Xu, et al.. Quasi-1D Polymer Semiconductor–Diarylethene Blends: High Performance Optically Switchable Transistors. *Advanced Functional Materials*, 2023, 33 (46), 10.1002/adfm.202305494 . hal-04278339

**HAL Id: hal-04278339**

**<https://hal.science/hal-04278339v1>**

Submitted on 9 Nov 2023

**HAL** is a multi-disciplinary open access archive for the deposit and dissemination of scientific research documents, whether they are published or not. The documents may come from teaching and research institutions in France or abroad, or from public or private research centers.

L'archive ouverte pluridisciplinaire **HAL**, est destinée au dépôt et à la diffusion de documents scientifiques de niveau recherche, publiés ou non, émanant des établissements d'enseignement et de recherche français ou étrangers, des laboratoires publics ou privés.

# Quasi-1D Polymer Semiconductor–Diarylethene Blends: High Performance Optically Switchable Transistors

Yusheng Chen, Hanlin Wang, Hu Chen, Weimin Zhang, Shunqi Xu, Michael Pätzel, Chun Ma, Cang Wang, Iain McCulloch, Stefan Hecht, and Paolo Samorì\*


Optically switchable field-effect transistors (OSFETs) are non-volatile photonic memory devices holding a great potential for applications in optical information storage and telecommunications. Solution processing of blends of photochromic molecules and  $\pi$ -conjugated polymers is a low-cost protocol to integrate simultaneously optical switching and charge transport functions in large-area devices. However, the limited reversibility of the isomerization of photochromic molecules due to steric hindrance when embedded in ordered polymeric matrices represents a severe limitation and it obliges to incorporate as much as 20% in weight of the photochromic component, thereby drastically diluting the electronic function, limiting the device performance. Herein, a comparative study of the photoresponsivity of a suitably designed diarylethene molecule is reported when embedded in the matrix of six different polymer semiconductors displaying diverse charge transport properties. In particular, this study focuses on three semi-crystalline polymers and three quasi-1D polymers. It is found that 1% w/w of 1,2-bis(5-(3,5-di-tert-butylphenyl)-2-methylthiophen-3-yl)cyclopent-1-ene in a blend with poly(indacenodithiophene-co-benzothiadiazole) is sufficient to fabricate OSFETs combining photo-modulation efficiencies of 45.5%, mobilities  $>1 \text{ cm}^2 \text{ V}^{-1} \text{ s}^{-1}$ , and photo-recovered efficiencies of 98.1%. These findings demonstrate that quasi-1D polymer semiconductors, because of their charge transport dominated by intra-molecular processes, epitomize the molecular design principles required for the fabrication of high-performance OSFETs.

## 1. Introduction

During the last decade, the controlled incorporation of functional molecules in semiconducting matrices has been demonstrated as a powerful approach to fabricate multifunctional devices. Such a strategy is particularly suitable when employing photochromic molecules for the development of light-responsive and thus optically controllable and programmable electrical devices. In this context, hybrids comprising azobenzene,<sup>[1–5]</sup> spiropyran,<sup>[6–11]</sup> and diarylethene<sup>[12–15]</sup> have garnered great attention for application in data storage, imaging, and sensing. Among them, diarylethenes (DAEs) have particular advantages since they can undergo reversible isomerization between the open and the closed states when irradiated with UV and visible (Vis) light, respectively. While the two states are thermally stable at ambient conditions, they exhibit vastly different energy levels of their frontier molecular orbitals, i.e., the lowest unoccupied molecular orbital (LUMO) and the highest occupied molecular orbital (HOMO).<sup>[16]</sup> Thus, DAEs are particularly adapted for optically modulating charge transfer in

Y. Chen, H. Wang, S. Xu, C. Ma, C. Wang, P. Samorì  
Université de Strasbourg  
CNRS  
ISIS  
8 allée Gaspard Monge, 67000 Strasbourg, France  
E-mail: samori@unistra.fr

H. Chen  
School of Physical Sciences  
Great Bay University  
Dongguan 523000, China

 The ORCID identification number(s) for the author(s) of this article can be found under <https://doi.org/10.1002/adfm.202305494>

© 2023 The Authors. Advanced Functional Materials published by Wiley-VCH GmbH. This is an open access article under the terms of the Creative Commons Attribution License, which permits use, distribution and reproduction in any medium, provided the original work is properly cited.

DOI: 10.1002/adfm.202305494

W. Zhang, I. McCulloch  
Physical Sciences and Engineering Division  
KAUST Solar Center (KSC)  
King Abdullah University of Science and Technology (KAUST)  
KSC Thuwal 23955-6900, Saudi Arabia

M. Pätzel, S. Hecht  
Department of Chemistry & IRIS Adlershof  
Humboldt-Universität zu Berlin  
Brook-Taylor-Str. 2, 12489 Berlin, Germany

I. McCulloch  
Department of Chemistry  
University of Oxford  
Oxford OX1 3TA, UK

blends with organic semiconductors upon irradiation at distinct wavelengths. Optically switchable field-effect transistors (OSFETs) based on DAEs combined with different  $\pi$ -conjugated polymer matrices featuring various microstructures and molecular weight have been thoroughly studied. Undoubtedly,  $\pi$ -conjugated polymers with a lower degree of crystallinity are favorable candidates for OSFETs, since crystalline polymer matrices can sterically hinder the switching process of the photochromic molecules leading to irreversible photoisomerizations and low photo-recovered efficiencies (PRE).<sup>[17–19]</sup> However, the use of less ordered  $\pi$ - $\pi$  stacked assemblies based on amorphous polymers determined a lower efficiency in the intermolecular charge transport, resulting in lower mobilities characterizing the previously reported OSFET devices.<sup>[20,21]</sup> Therefore, finding a trade-off between these two opposing effects, i.e., high PRE and high device mobility (exceeding  $0.1 \text{ cm}^2 \text{ V}^{-1} \text{ s}^{-1}$ ), is highly sought after and it represents a major challenge in OSFETs research.<sup>[22,23]</sup> Moreover, the use of high amount of DAEs in the active blend has two opposite effects: it offers an increased light-gating effect yet it yields a major decrease in the device mobility compared with the pristine polymer. In previously reported OSFETs, to achieve high photo-modulation efficiencies (PMEs), as much as 20% in weight of DAE in polymer matrices was utilized because of the small energy offset ( $<0.4 \text{ eV}$ ) between the HOMO of closed DAEs and polymers, yielding a loss of device mobility of  $\approx 50\%$ .<sup>[24]</sup> However, one can expect that the selection of DAE and polymers with a larger energy offset can enable high photo-modulation also upon using a smaller relative amount of DAE, thereby imposing a minimal decrease in the device mobility.

Notably, most of the building blocks used in D-A conjugated polymer, i.e., diketopyrrolopyrrole (DPP), (E)-1,2-bis(3,4-difluorothien-2-yl)ethene (TVT), and 2,2'-bithiophene (TT), display a high degree of conformational flexibility as evidenced by their tendency to undergo bending, chain folding, entanglement, or twisting out of coplanarity thus yielding insufficient intramolecular charge transport. Conversely, long-range  $\pi$ -conjugated polymers, named quasi-1D polymers, display sufficient intramolecular charge transport through their rigid  $\pi$ -conjugated backbone, which is achieved by embedding fuse-ring repeating units and by introducing non-covalent interactions between the building blocks.<sup>[25–29]</sup> Importantly, compared with branched alkyl chains on the  $\beta$  position, such as 2-ethylhexyl, 2-hexyldecyl, 2-octyldecyl, and 2-decyltetradecyl, the introduction of branched alkyl side chains on the backbone position in quasi-1D polymer yields a weaker tendency toward  $\pi$ - $\pi$  intermolecular stacking, leading a nearly-amorphous film morphology.<sup>[30]</sup> As a result, high field-effect mobilities and amorphous nature can be simultaneously obtained in quasi-1D polymer simultaneously. By devising unique structures comprising fused-rings of electron donor or acceptor building blocks, a series of quasi-1D polymers with mobilities approaching  $1 \text{ cm}^2 \text{ V}^{-1} \text{ s}^{-1}$  have been designed and synthesized.<sup>[31,32]</sup> While hitherto the performance of OSFET incorporating blends of DAEs and semiconducting polymers possessing different microstructures (amorphous, semi-crystalline, and highly crystalline) have been thoroughly investigated,<sup>[17]</sup> the use of DAEs blends with quasi-1D polymers, characterized by sufficient intramolecular charge

transport and amorphous morphology, has not been explored thus far and holds significant potential for boosting the device performance.

Aiming at developing OSFET displaying simultaneously extremely high PREs, high PME, and high field-effect mobilities, in this work we have blended photochromic DAEs with quasi-1D semiconducting polymers and revealed the effect of the DAEs switching on intramolecular charge transport within the conjugated polymer matrix (**Figure 1**). In particular, we have focused on poly(indacenodithiophene-co-benzothiadiazole) (IDT-BT) as archetypical quasi-1D polymer to uncover the molecular design guidelines for next-generation high-performance optically switchable transistors. To gain insight into the role of the chemical structure and rigidity of the  $\pi$ -conjugated backbone that can be expected to determine different intramolecular charge transport characteristics, we have extended our study to semi-crystalline polymers poly(diketopyrrolopyrrole-co-thiophene) (DPP3T). Both polymers were functionalized with different alkyl side chains that endow high solubility, yet they prevent ordered stacking if grafted directly to the backbone (**Figure 1a**).<sup>[33]</sup> The particular DAEs derivative, 1,2-bis(5-(3,5-di-tert-butylphenyl)-2-methylthiophen-3-yl)cyclopent-1-ene (DAEtBu), was chosen to exhibit a photo-induced modulation of its HOMO level to assure hole trapping in the closed but not in the open state (**Figure 1a,b**) and to avoid aggregation and thus phase separation of the photo-switchable component.<sup>[34]</sup> Comparative studies on the photochemical properties and morphology of polymer/DAEs blend film were carried out by UV-vis absorption spectroscopy and atomic force microscopy (AFM), respectively. OSFETs with various DAEs blending ratio were fabricated and characterized by investigating their response to the exposure to light at different wavelengths. Temperature-dependent measurement of OSFETs provided key insight into the charge transport mechanisms existing in the polymer/DAEs blend films. To attain a deeper understanding and demonstrate the general relevance of the use of quasi-1D polymers to attain high performance in OSFET, we have investigated two additional quasi-1D polymers with fused ring backbone structure, i.e., poly(thienoindenofluorene-co-benzothiadiazole) (TIF-BT) and poly(thiophenebenzo[b]indacenodithiophene-co-benzothiadiazole) (TBIDT-BT), and two further semi-crystalline polymers, i.e., poly(diketopyrrolopyrrole-co-benzothiadiazole) (DPPBT) and poly(diketopyrrolopyrrole-co-bithiophene) (DPP4T).

## 2. Results and Discussion

The chemical structures and respective energy levels of the six  $\pi$ -conjugated polymers and the chosen photochromic molecule are portrayed in **Figure 1a,b**. Among DAEs, we have focused our attention to DAEtBu because of its matching frontier molecular orbital energy levels, high reversibility and thus low fatigue during switching, and limited tendency to undergo aggregation because of its bulky side groups.<sup>[34]</sup> Moreover, the highest occupied molecular orbital (HOMO) values of DAEtBu in the open and closed isomer, amounting to  $-5.60$  and  $-4.80 \text{ eV}$ , respectively, are ideal in view of the HOMOs of the chosen polymers in order to attain photo-modulated charge transport in a process ruled by charge transfer. More specifically, the HOMO

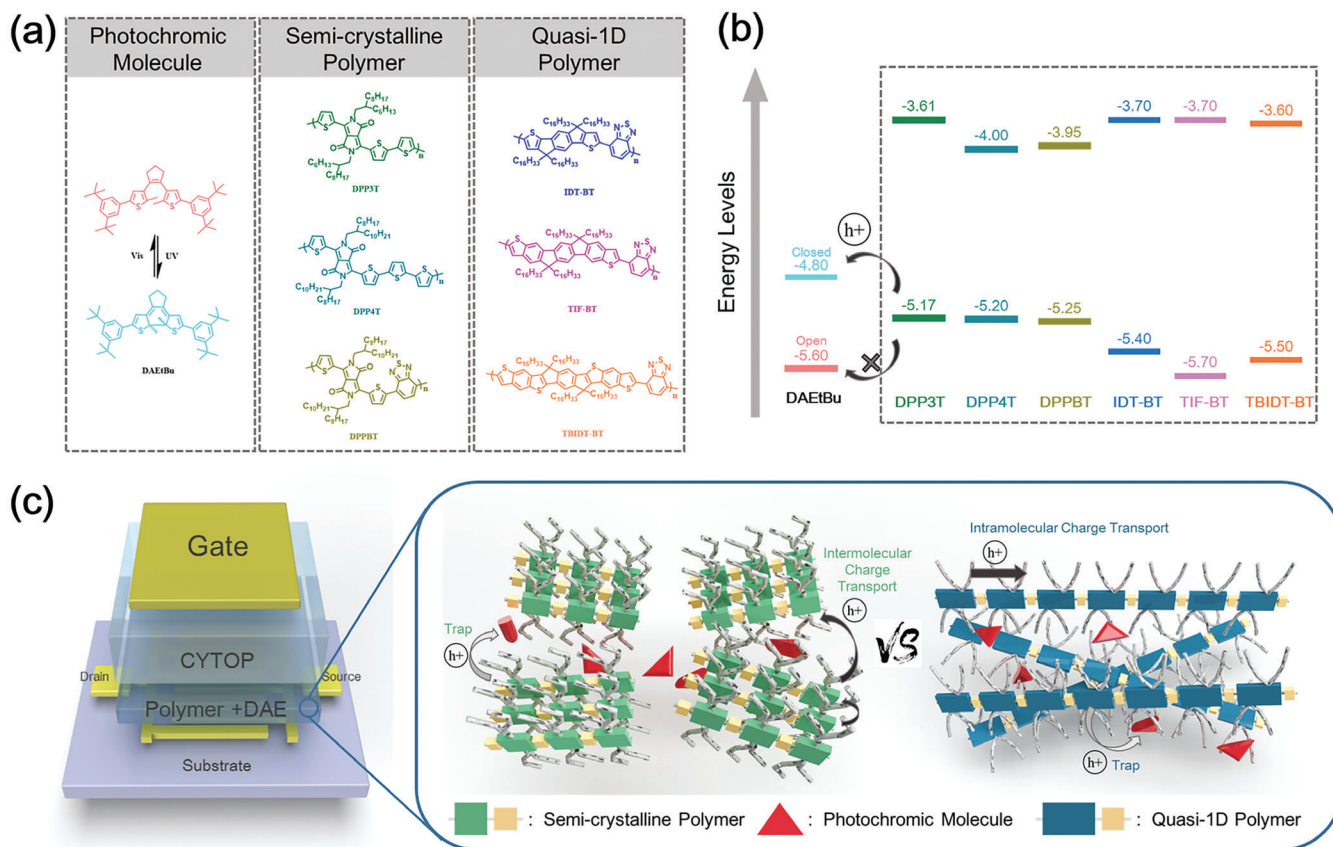


**Figure 1.** a) Chemical structures and b) energy levels of DAETBu molecule and six  $\pi$ -conjugated polymers used in this work. c) Device structure of optical switchable transistors including schematic illustration comparing the interactions involving the semi-crystalline versus quasi-1D polymers.

of the closed DAETBu falls in the bandgap of the semiconducting polymers, hence, the photochromic molecules act as traps for hole carriers transported through the polymer matrix. Instead, upon back-isomerization of the DAETBu's from the closed to the open isomer a de-trapping process takes place. As a result, multi-levels non-volatile readout current of the OSFETs is tuned by the isomerization of the DAETBu within the blend.<sup>[35]</sup>

OSFETs studied in this work were fabricated in a bottom contact/top-gate configuration (Figure 1c). To avoid dissolving DAETBu molecules at the air-solid interface, the dielectric layer of perfluoro(1-butenyl vinyl ether) polymer (CYTOP) was spin-coated on the top of the polymer/DAEs blend film by using a special fluorinated solvent, which is an orthogonal solvent for most common organic materials. UV light at  $\lambda = 312$  nm and Vis light at  $\lambda = 530$  nm were irradiated from the device's top through semi-transparent gold/CYTOP stacked layer. The optical characteristics of the gold/CYTOP stack are revealed in the spectrum attesting a transparency of 52% and 35% at 530 and 312 nm, respectively (see Figure S1a, Supporting Information). The dielectric constant of CYTOP was defined in the sandwich structure of Si/CYTOP/Au. Capacitance-frequency curves of these devices (see Figure S1b, Supporting Information) provide a CYTOP's capacitance of  $1.8 \text{ nF cm}^{-2}$ .

## 2.1. Photochemical Properties and Morphology of Polymer/DAETBu Blend Films

The photochemical isomerization of DAETBu as monocomponent film and when embedded in the polymer matrixes of DPP3T and IDT-BT has been investigated by UV-vis absorption spectroscopy. The resulting UV-vis spectra of DAETBu neat film (Figure S2a, Supporting Information) reveal successful isomerization of DAETBu from the open to the closed isomer upon UV irradiation (312 nm for 5 min), yielding a new broad absorbance feature between 400 and 650 nm. Full reversibility to the initial spectra is achieved upon irradiation with visible light (530 nm for 10 min) by triggering the back-isomerization from the closed to the open isomer. The comparative study on the photo-isomerization of DAETBu when embedded in DPP3T and IDT-BT was carried out by exploiting the same irradiation power and exposure time, in a polymer:DAETBu blend film with a 90%:10% weight ratio supported on quartz substrate (Figure 2). For the sake of comparison, spectroscopic analysis of the neat polymer films has been carried out as well and the spectra did not show any significant shift when mixed with DAETBu, suggesting a minor influence of the bending on the  $\pi$ - $\pi$  stacking between adjacent polymer chains (see Figure S2b, Supporting Information). Absorbance value changes in bi-component films



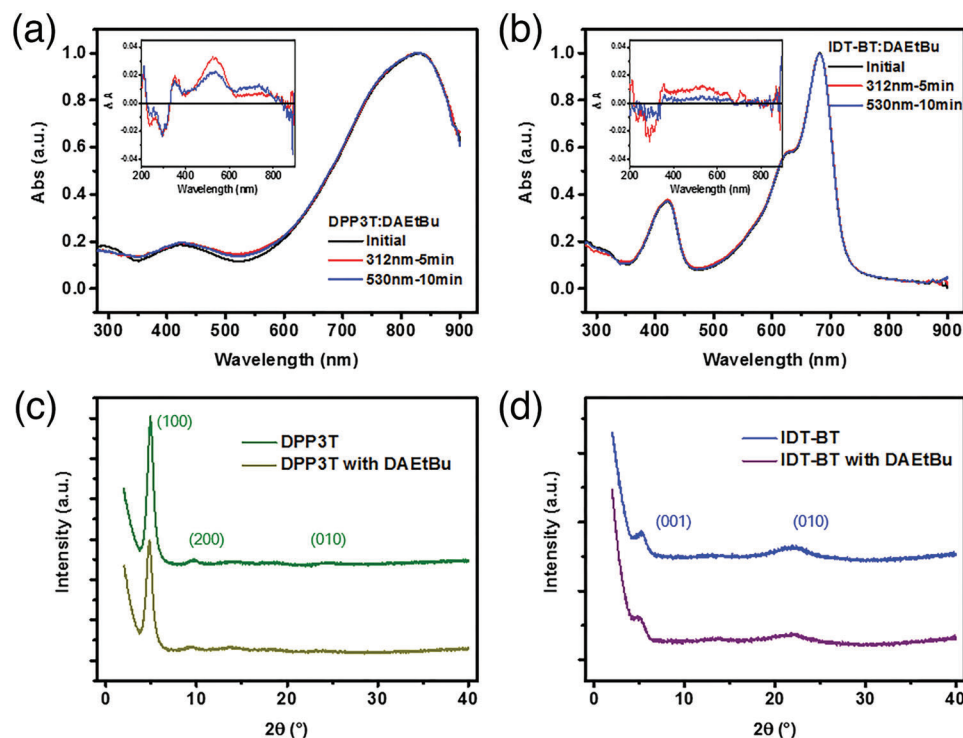


**Figure 2.** UV-vis absorption spectra of a) DPP3T/DAEBu blend film and b) IDT-BT/DAEBu blend film upon UV light irradiation and visible irradiation. The inset presents the differential changes in absorbance after light irradiation. c) In-plane X-ray diffraction of DPP3T neat film and DPP3T:DAEBu bi-component film. d) In-plane X-ray diffraction of IDT-BT neat film and IDT-BT:DAEBu bi-component film.

subjected to light irradiation are portrayed in the inset of Figure 2. When irradiated with UV light both bi-component films display slightly enhanced absorbance at 530 nm accompanied by reduced absorbance at 312 nm, indicating the formation of the closed DAEBu isomer. However, when subsequently exposed to visible light these two blend films display a different degree of absorbance recovery, which is evident from the change in the absorption coefficient at 530 nm. In particular, upon irradiation with 530 nm light, the DPP3T based blend exhibited a limited recovery (i.e., 30%), whereas the IDT-BT based blend recovered to much larger extent (i.e., 75%). These results indicate that the steric hindrance brought into play by the tighter packing within the DPP3T films hinders the DAEBu's back-isomerization from closed to open isomer. Such a steric hindrance is limited when IDT-BT is employed, yielding a more efficient recovery of the open state.

In-plane X-ray diffraction (XRD) analysis was carried out to elucidate the molecular packing and crystalline microstructure of polymer/DAEBu drop-cast thin film, as shown in Figure 2c,d. A strong diffraction peak for DPP3T neat film was observed at  $2\theta = 4.8^\circ$ , corresponding to 1.84 nm lamellar stacking distance along the alkyl side chain direction (100).<sup>[36]</sup> Conversely, in stark contrast with semi-crystalline microstructure in DPP3T neat film, the neat IDT-BT films revealed the absence of the (100) peak at  $2\theta = 3.9^\circ$  but a clear (001) peak at  $2\theta = 5.3^\circ$ , suggesting an intramolecular order that endow efficient charge transport along the repeating unit of backbone with a length of 1.66 nm.<sup>[30]</sup> Bi-component films containing 10% w/w of DAEBu show a subtle shift ( $\approx 0.1^\circ$ ) of the DPP3T (100) diffraction peak and the IDT-

BT (001) diffraction peak, indicating that the microstructure of the polymer matrices were only mildly disrupted upon addition of the photochromic molecule. The assembly of the neat polymers and respective bi-component films at increasing content of DAEBu was investigated by AFM. **Figure 3** displays a rather flat grain-like morphology not evidencing the presence of a significant phase separation between the polymer and DAEBu component. The root-mean squared ( $R_{\text{RMS}}$ ) roughness of these films was estimated in region of  $5 \times 5 \mu\text{m}^2$ . The  $R_{\text{RMS}}$  of neat films of DPP3T and IDT-BT amounts to 0.42 and 0.51 nm, while the  $R_{\text{RMS}}$  of blended films of DPP3T/DAEBu (10%) and DPP3T/DAEBu (10%) provides  $R_{\text{RMS}}$  values of 0.37 and 0.38 nm. This subtle decrease in the  $R_{\text{RMS}}$  indicates that the DAEBu molecules fill the void space within the polymer matrix. Both the XRD and AFM results demonstrate the good miscibility between the polymers and DAEBu, which is key to secure efficient physical and energetic interaction between the two components, hence being advantageous for efficient current photo-modulation in the OSFET devices.

## 2.2. Electrical Properties of OSFETs

The electrical properties of the DPP3T and IDT-BT monocomponent films and their blends with DAEBu were investigated by fabricating OSFETs in a bottom contact/top-gate configuration. The channel length and width amounted to 200 and 20 nm, respectively. Transfer curves of both DPP3T and IDT-BT based devices are displayed in Figures S3 and S4 (Supporting

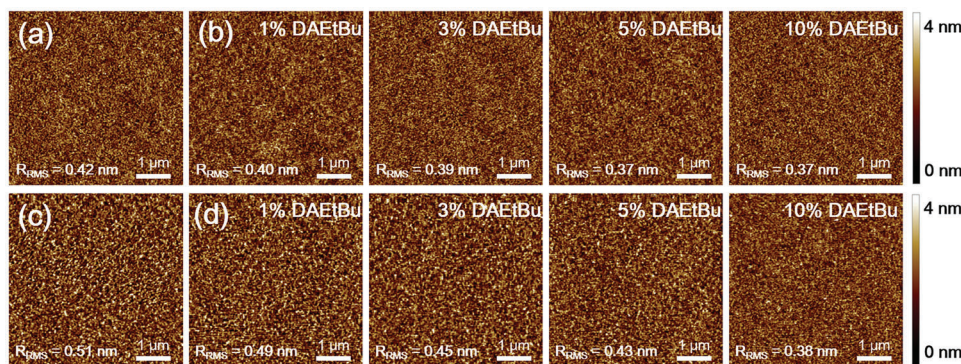


**Figure 3.** Morphology of a) DPPBT neat film and b) DPPBT/DAEBu blend films with various blended ratio. c) IDT-BT neat film and d) IDT-BT/DAEBu blend films with various blended ratio.

Information). The control devices comprising neat DPP3T and IDT-BT films did not exhibit any current photo-modulation upon irradiation with UV and Vis light. DAEBu was then added into DPP3T and IDT-BT films with increasing weight ratio (at 1%, 3%, 5–10%). Although the mobility of DPP3T and IDT-BT based films is similar, the photo-switching behavior is completely different (Figure 4a,b). After the first 5 min irradiation with UV (312 nm) light, the drain-source current ( $I_{DS}$ ) of all devices decreased significantly, because the UV triggered ring-closure of DAEBu, whose HOMO level act as trap level for the holes of the semiconductor. For DPP3T-based devices, 1%, 3%, 5%, and 10% closed DAEBu in the blended film led to PME values of 28.1%, 40.9%, 61.0%, and 73.4%, respectively. In contrast, the same amounts of 1%, 3%, 5%, and 10% closed DAEBu blended in

IDT-BT-based devices increase the PME to 45.5%, 87.5%, 92.3%, and 97.9%, respectively. The general trend of increasing PME with increasing DAEBu content correlates with the greater number of traps generated by irradiation within the film. Interestingly, IDT-BT-based devices exhibited excellent PMEs even with a minimal content of the photochromic molecule, i.e., 1% and 3%. Such a result can be attributed to the larger HOMO level gap (>0.6 eV) between IDT-BT and closed DAEBu. On the other hand, visible light irradiation for 10 min at  $\lambda = 530$  nm of the DPP3T-based devices showed only a modest recovery of  $I_{DS}$ , presumably due to the sterically hindered back-isomerization of DAEBu embedded into the ordered polymer matrixes, overall resulting in decreasing field-effect mobilities. Conversely, upon visible light irradiation, the 1% and 3% DAEBu blend IDT-BT-based devices

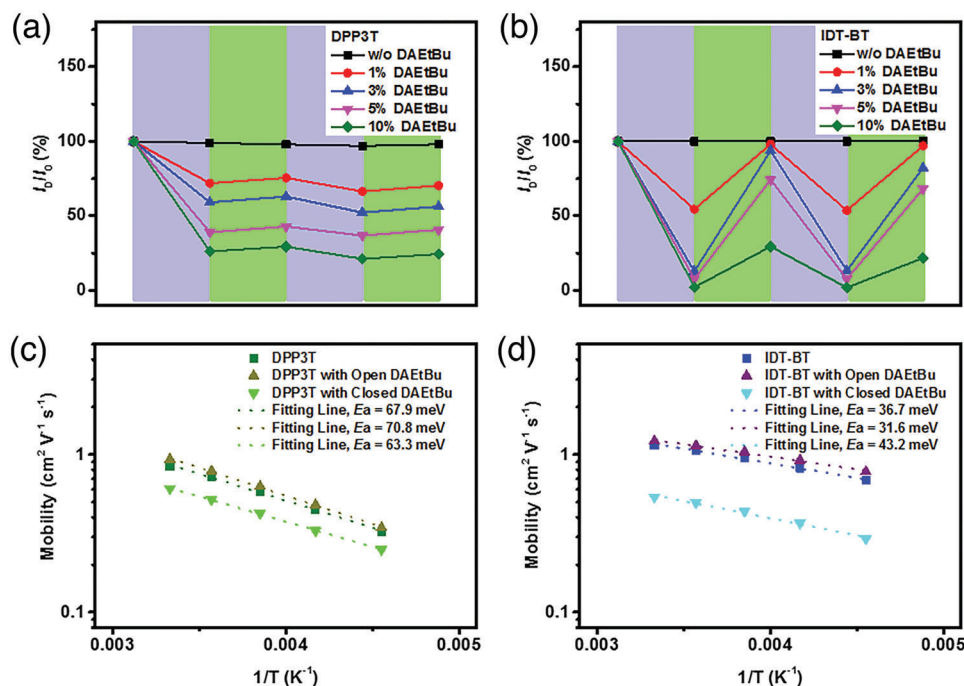


**Figure 4.** Reversible modulation of drain-source current through blends of a) DPP3T/DAEBu, and b) IDT-BT/DAEBu based OSFETs upon cycling UV (312 nm, violet shaded areas) and visible light irradiation (530 nm, green shaded areas) at  $V_G = V_D = -60$  V. An Arrhenius plot of c) IDT-BT-based devices and d) DPP3T-based devices.

displayed a nearly full recovery of the initial  $I_{DS}$ , as attested by PRE values of 98.1% and 93.8%, combined with excellent mobilities of over  $1 \text{ cm}^2 \text{ V}^{-1} \text{ s}^{-1}$  for both 1% and 3% DAEBu blended IDT-BT-based devices, fulfilling the requirement for a practical application. In the IDT-BT-based devices, increasing the amount of DAEBu up to 5% and 10% caused a lowering of the PRE to 74.3% and 29.5%, respectively. Such observations can contribute to a steric hindrance on the DAEBu switching determined by the limited crystalline nature of the IDT-BT matrix, which leads to an irreversible light responsiveness of the current in the device thus also a lower PRE. Expectedly, upon a further second UV/Vis light irradiation cycle, in the 1% and 3% DAEBu blended IDT-BT-based device, relatively high PRE with values of 97.0% and 82.2% were achieved. Compared with the PRE value in first light irradiation cycle, lower PRE in second cycle of all the devices indicated charge transport in the thin film potentially influenced by the formation of the photochemically irreversible cycloannulated isomer of DAEBu.<sup>[37]</sup> To further investigate the photo-stability of IDT-BT/DAEBu based OSFETs, the normalized  $I_{DS}$  taken from the transfer curves obtained during ten measured cycles was plotted in the Figure S5 (Supporting Information).<sup>[38,39]</sup> After ten cycles of photo irradiation, the IDT-BT/DAEBu based OSFETs retain the photo-switching behavior with PME of 91.5% and PRE of 61.0%, providing evidence for a high photo-stability.

To elucidate this different photo-switching behavior, temperature-dependent electrical characterizations were carried out, as shown in Figures S6 and S7 (Supporting Information). The mobilities at different temperatures (220–300 K) were extracted as described above and are shown in an Arrhenius plot (Figure 4c,d), which allowed to quantify the activation energy ( $E_A$ ) of 67.9 and 36.7 meV for DPP3T and IDT-BT, respectively. The device mobility is a quantification of charge transport rate in organic semiconductors. In conjugated macromolecules the charge transport depends on both intermolecular and intramolecular thermally activated electron hopping. The mobility of devices depends on temperature as expressed by  $\mu \approx \exp(-E_A/k_b T)$ , where  $k_b$  and  $T$  are the Boltzmann constant, and temperature, respectively. The intramolecular charge transport in localized  $\pi$ -molecular orbitals needs to overcome the energy barrier due to the hopping between adjacent repeating units. However, twisted, entangled, and folded molecular chains in conjugated polymer lead an energetic disorder of the molecular orbital, resulting in larger energy barriers required in intermolecular charge transport.<sup>[40–43]</sup> Extremely low  $E_A$  observed in the IDT-BT-based devices indicates the predominance of intramolecular charge transport within the polymer matrix when compared to the case of DPP3T polymer. Upon blending with 3% open or closed DAEBu, the  $E_A$  of both blends displayed only a subtle change, amounting to 70.8 meV/63.3 meV and 31.6 meV/43.2 meV in DPP3T and IDT-BT based devices, respectively, which suggests the charge transport behavior is just barely influenced by the DAEBu present, regardless of its open isomer or closed isomer. Moreover, the current successfully modulation in DPP3T-based and IDT-BT-based device provides unambiguous evidence that photochromic DAEBu molecule can photo-modulate both intermolecular and intramolecular charge transport.

### 2.3. Versatile OSFETs with Quasi-1D Polymers

To draw general conclusions on the photo-switching behavior of DAEs when embedded in matrices of semi-crystalline or quasi-1D polymers, OSFETs based on DPPBT, DPP4T, TIF-BT, and TBIDT-BT were fabricated and measured, keeping a DAEBu blend weight ratio of 3%. The morphologies of the neat polymer films and their blend with DAEBu were monitored by AFM (Figures S8–S11, Supporting Information) and the respective transfer curves measured (Figures S12 and S13, Supporting Information). Importantly, Figure 5 shows that the photo-switching behavior of semi-crystalline polymers and quasi-1D polymer-based blends is remarkably different. OSFET devices comprising DPPBT and DPP4T exhibit an irreversible  $I_{DS}$  after 10 min visible light irradiation, with PRE of 26.4% and 42.0%, respectively. Noteworthy, when compared with IDT-BT, donor–acceptor conjugated polymer DPPBT contains the same acceptor unit but different donor moiety, demonstrating that a large fuse-ring backbone structure is a key feature for optimal material design in OSFETs. On the contrary, superior PREs with values of 51.5% and 73.7% were obtained in TIF-BT-based and TBIDT-BT-based OSFETs, respectively. In the second irradiation cycles, PRE of 30.2% and 59.2% were recorded. Furthermore, the large energy level gap ( $>0.7 \text{ eV}$ ) between the closed DAEBu and the polymer TIF-BT/TBIDT-BT leads to the highest PME of 94.3%/99.9%. Correspondingly, due to the small energy level gap ( $<0.1 \text{ eV}$ ) between the HOMO levels of open DAEBu and that of both TIF-BT and TBIDT-BT, the mobility of TIF-BT-based and TBIDT-BT-based OSFETs decreased after blending from  $1.09$  to  $0.77 \text{ cm}^2 \text{ V}^{-1} \text{ s}^{-1}$  and  $0.50$  to  $0.30 \text{ cm}^2 \text{ V}^{-1} \text{ s}^{-1}$ , respectively. Instead, a small mobility decreases from  $1.35$  to  $1.14 \text{ cm}^2 \text{ V}^{-1} \text{ s}^{-1}$  was observed in IDT-BT blend-based devices containing 3% of DAEBu. In fact, the position of the HOMO levels of IDT-BT is ideal for OSFETs application. More precisely, it exhibits a maximum energy gap ( $0.6 \text{ eV}$ ) between IDT-BT and closed DAEBu to guarantee sufficient PME combined with a small energy gap ( $0.2 \text{ eV}$ ) between IDT-BT and open DAEBu, thereby preventing the occurrence of thermal activated charge carrier trapping hence not significantly affecting the device mobility of the pristine polymer. All the most relevant parameters characterizing these devices are provided in Table 1 and Table S1 (Supporting Information). They reveal that the optical response brought into play by the presence of DAEBu in the polymer matrix significantly affects the device mobility, whereas it has a minor influence on all other device parameters.

### 3. Conclusion

The blending of a photochromic diarylethene with different polymeric semiconductors was employed to increase the functional complexity of organic field-effect transistors by imparting them with reversible optical switchability. In order to simultaneously maximize the device mobility, PME, and PRE, we have carried out an in-depth investigation of the performance of a previously optimized DAEs blended with high mobility  $\pi$ -conjugated polymers featuring two types of microstructures. We found that the DAEs are capable of trapping charge carriers not only participating to intermolecular transport processes, but also to intramolecular ones. Hence, polymers displaying a limited



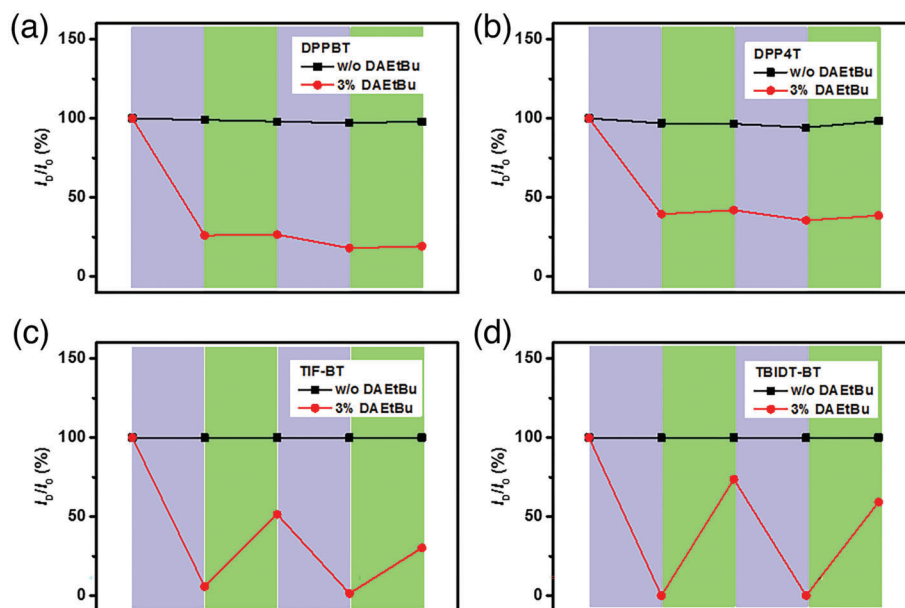


**Figure 5.** Reversible modulation of drain-source current of a) DPPBT/DAEtBu based, b) DPP4T/DAEtBu based, c) TIF-BT/DAEtBu based and d) TBIDT-BT/DAEtBu based OSFETs over irradiation cycles with UV irradiation (312 nm, violet shaded areas) and visible irradiation (530 nm, green shaded areas) at  $V_G = V_D = -60$  V.

propensity to form crystalline assemblies and extended planar fuse-ring structures represent better candidates for the fabrication of high-performance OSFETs. Upon comparing a series of quasi-1D polymers combined with DAEtBu, we found that IDT-

BT is the ideal polymer in view of its HOMO level with respect to the HOMO of the open and closed state of the photochrome. As a result, high performance optical switchable transistors with mobility of  $1.16 \text{ cm}^2 \text{ V}^{-1} \text{ s}^{-1}$ , PME of 45.5% and PRE of 98.1% were realized based on solution processing of blends of IDT-BT and DAEtBu forming thin films. Such an understanding over the microstructure and energy level versus current photo-switching behavior is of general applicability to n-type and ambipolar quasi-1D polymer/DAEs-based OSFETs.<sup>[44–46]</sup> This universal strategy represents a major step forward in OFETs and is highly relevant also for the development of FETs capable to respond to other external stimuli via the controlled interfacing of the conjugated polymer with functional molecules imparting the responsiveness of interest, toward future rational design of multifunctional materials and devices.

**Table 1.** Summary of key parameters of OSFETs.

System		Initial Mobility [ $\text{cm}^2 \text{ V}^{-1} \text{ s}^{-1}$ ]	Roughness [nm]	PME [%] <sup>a)</sup>	PRE [%] <sup>b)</sup>	
					1st cycle	2nd cycle
DPP3T	w/o DAEtBu	0.75	0.42	–	–	–
	1% DAEtBu	0.90	0.40	28.1	75.5	70.4
	3% DAEtBu	0.97	0.39	40.9	63.0	56.3
	5% DAEtBu	1.01	0.37	61.0	42.9	40.7
	10% DAEtBu	1.18	0.37	73.4	29.4	24.4
IDT-BT	w/o DAEtBu	1.35	0.51	–	–	–
	1% DAEtBu	1.16	0.49	45.5	98.1	97.0
	3% DAEtBu	1.14	0.45	87.5	93.8	82.2
	5% DAEtBu	0.87	0.43	92.3	74.3	68.2
	10% DAEtBu	0.85	0.38	97.9	29.5	21.7
DPPBT	w/o DAEtBu	0.090	1.28	–	–	–
	3% DAEtBu	0.094	0.59	74.1	26.4	19.1
DPP4T	w/o DAEtBu	0.69	1.60	–	–	–
	3% DAEtBu	0.69	1.34	60.4	42.0	38.5
TIF-BT	w/o DAEtBu	1.09	0.88	–	–	–
	3% DAEtBu	0.77	0.61	94.3	51.5	30.2
TBIDT-BT	w/o DAEtBu	0.50	2.54	–	–	–
	3% DAEtBu	0.30	0.96	99.9	73.7	59.2

<sup>a)</sup> The PME value was calculated by estimating the percentage of UV-reduced  $I_{DS}$  versus initial  $I_{DS}$ . <sup>b)</sup> The PRE value was calculated by estimating the percentage of Vis-recorded  $I_{DS}$  versus initial  $I_{DS}$ .

## 4. Experimental Section

**Materials:** All  $\pi$ -conjugated polymers and photochromic molecules were synthesized according to the reported procedures.<sup>[16,47–50]</sup> The molecular weight ( $M_n/M_w$ ) of DPP3T, DPP4T, DPPBT, IDT-BT, TIF-BT, and TBIDT-BT is 34.7k/63.9k, 43.0k/75.3k, 55.0k/88.7k, 103k/245k, 87k/178k, and 82k/212k, respectively. Anhydrous chlorobenzene was purchased from Sigma–Aldrich. CYTOP (CTL-809 m; Asahi Glass) solution was purchased from AGC Chemicals Europe Ltd.

**Solution Preparation:** Sixty milligrams of  $\pi$ -conjugated polymers were dissolved in 10 mL of chlorobenzene, and then stirred at 80 °C overnight. Sixty milligrams of photochromic molecule DAEtBu were dissolved in 10 mL of chlorobenzene. DAEtBu-doping polymer solutions (1%, 3%, 5%, and 10%) were prepared from mixing 100 mL polymer solution with 1 mL, 3 mL, 5 mL, and 10 mL DAEtBu solution, respectively. All solutions were prepared in a nitrogen filled glovebox.

**Characterization of Thin Films:** The samples for UV/vis absorption spectra measurement were prepared by spin-coating the solution on clean



quartz, and the spectra were recorded on JASCO V-650 spectrophotometer. Device irradiation was realized by using a monochromator set-up, with either UV light (at  $\lambda = 312$  nm,  $0.3$  mW cm<sup>-2</sup>) or green light ( $\lambda = 530$  nm,  $10$  mW cm<sup>-2</sup>). AFM images were recorded with a Bruker Dimension Icon set-up operating under ambient conditions, in tapping mode. XRD patterns were collected by the Bruker D8 ADVANCE diffractometer on silicon substrate and irradiation wavelength of X-ray is  $0.15418$  nm. The d-spacing distance was estimated by Bragg's law.

**Fabrication and Characterization of Optical Switchable Transistors:** Devices were fabricated in a bottom contact/top-gate configuration, on the substrates of ultra-flat glass (Ossila Company). The ultra-flat glass substrates were cleaned with water, acetone, and alcohol in sequence and dried under N<sub>2</sub> flow. The cleaned was further treated with UV-ozone for 20 min. Interdigitated Cr/Au electrodes (1/25 nm) were deposited on the glass substrates through shadow masks. Subsequently, the DAETBu-doping polymer solution and neat polymer solution were spin-coated at 1800 rpm for 1 min on the glass, and then dried at 90 °C for 10 min to get blending film and neat film. Dielectric layer with thickness of 1  $\mu$ m was spun from CYTOP solution, followed by a thermal annealing at 90 °C for 10 min. A Gold electrode with thickness of 30 nm was deposited through shadow masks. Devices were characterized in a dry and nitrogen-filled glove box. The electric characteristics were measured by a semiconductor parameter analyzer (Keithley 2636). Temperature dependence measurements were carried out in a customized Janis cryogenic probe station, combined with a semiconductor parameter analyzer (Keithley 4200A SCS). The chamber pressure was kept at  $\approx 10^{-5}$  Pa and the error of temperature measurement was  $\pm 0.2\%$ .

## Supporting Information

Supporting Information is available from the Wiley Online Library or from the author.

## Acknowledgements

This work was financially supported by the Agence Nationale de la Recherche through the Interdisciplinary Thematic Institute SysChem via the IdEx Unistra (ANR-10-IDEX-0002) within the program Investissement d'Avenir, the Foundation Jean-Marie Lehn, the Institut Universitaire de France (IUF), the Chinese Scholarship Council, and the German Research Foundation (DFG via project 182087777 – SFB 951). H.C. acknowledges the financial support from the open research fund of the Songshan Lake Materials Laboratory (2022SLABFN06), Dongguan, China. I.M. acknowledges financial support from KAUST Office of Sponsored Research CRG10, by EU Horizon2020 grant agreement no. 952911, BOOSTER, grant agreement no. 862474, RoLA-FLEX, and grant agreement no. 101007084 CITYSOLAR, as well as EPSRC Projects EP/T026219/1 and EP/W017091/1.

## Conflict of Interest

The authors declare no conflict of interest.

## Data Availability Statement

The data that support the findings of this study are available from the corresponding author upon reasonable request.

## Keywords

optical switchable transistors, photochromic molecules, quasi-1D polymers

Received: May 19, 2023  
Revised: June 28, 2023  
Published online: July 12, 2023

- [1] J. Tian, L. Fu, Z. Liu, H. Geng, Y. Sun, G. Lin, X. Zhang, G. Zhang, D. Zhang, *Adv. Funct. Mater.* **2019**, *29*, 1807176.
- [2] A. Galanti, J. Santoro, R. Mannancherry, Q. Duez, V. Diez-Cabanes, M. Valasek, J. De Winter, J. Cornil, P. Gerbaux, M. Mayor, P. Samori, *J. Am. Chem. Soc.* **2019**, *141*, 9273.
- [3] A. K. Bartholomew, I. B. Stone, M. L. Steigerwald, T. H. Lambert, X. Roy, *J. Am. Chem. Soc.* **2022**, *144*, 16773.
- [4] H. Peng, J. C. Qi, X. J. Song, R. G. Xiong, W. Q. Liao, *Chem. Sci.* **2022**, *13*, 4936.
- [5] H. F. Drake, Z. Xiao, G. S. Day, S. W. Vali, L. L. Daemen, Y. Cheng, P. Cai, J. E. Kuszynski, H. Lin, H. C. Zhou, M. R. Ryder, *ACS Appl. Mater. Interfaces* **2022**, *14*, 11192.
- [6] A. V. Mumyatov, L. A. Frolova, L. G. Gutsev, E. A. Khakina, N. A. Sanina, S. M. Aldoshin, P. A. Troshin, *J. Mater. Chem.* **2023**, *11*, 963.
- [7] C. F. Liu, H. Lin, S. S. Li, H. Xie, J. L. Zhang, D. Z. Ji, Y. Yan, X. Liu, W. Y. Lai, *Adv. Funct. Mater.* **2022**, *32*, 2111276.
- [8] M. B. Leinen, P. Klein, F. L. Sebastian, N. F. Zorn, S. Adamczyk, S. Allard, U. Scherf, J. Zaumseil, *Adv. Electron. Mater.* **2020**, *6*, 2000717.
- [9] C. Li, A. Iscen, L. C. Palmer, G. C. Schatz, S. I. Stupp, *J. Am. Chem. Soc.* **2020**, *142*, 8447.
- [10] H. G. Jang, J. Y. Jo, H. Park, Y. C. Jung, Y. S. Choi, S. Jung, D. C. Lee, J. Kim, *Adv. Mater.* **2022**, *8*, 2200566.
- [11] M. Reifarh, M. Bekir, A. M. Bapolisi, E. Titov, F. Nusshardt, J. Nowaczyk, D. Grigoriev, A. Sharma, P. Saalfrank, S. Santer, M. Hartlieb, A. Böker, *Angew. Chem., Int. Ed.* **2022**, *61*, 202114687.
- [12] Z. Zhang, W. Wang, P. Jin, J. Xue, L. Sun, J. Huang, J. Zhang, H. Tian, *Nat. Commun.* **2019**, *10*, 4232.
- [13] S. A. Diaz, F. Gillanders, E. A. Jares-Erijman, T. M. Jovin, *Nat. Commun.* **2015**, *6*, 6036.
- [14] G. Ligorio, G. F. Cotella, A. Bonasera, N. Zorn Morales, G. Carnicella, B. Kobin, Q. Wang, N. Koch, S. Hecht, E. J. W. List-Kratochvil, F. Cacialli, *Nanoscale* **2020**, *12*, 5444.
- [15] A.-K. Steppert, A. Mikosch, T. Haraszti, R. Göstl, A. J. C. Kuehne, *ACS Photonics* **2019**, *6*, 558.
- [16] M. Herder, B. M. Schmidt, L. Grubert, M. Pätzl, J. Schwarz, S. Hecht, *J. Am. Chem. Soc.* **2015**, *137*, 2738.
- [17] L. Hou, T. Leydecker, X. Zhang, W. Rekab, M. Herder, C. Cendra, S. Hecht, I. McCulloch, A. Salleo, E. Orgiu, P. Samori, *J. Am. Chem. Soc.* **2020**, *142*, 11050.
- [18] M. Carroli, D. T. Duong, E. Buchaca-Domingo, A. Liscio, K. Börjesson, M. Herder, V. Palermo, S. Hecht, N. Stingelin, A. Salleo, E. Orgiu, P. Samori, *Adv. Funct. Mater.* **2020**, *30*, 1907507.
- [19] M. Carroli, A. G. Dixon, M. Herder, E. Pavlica, S. Hecht, G. Bratina, E. Orgiu, P. Samori, *Adv. Mater.* **2021**, *33*, 2007965.
- [20] C. Wang, H. Dong, W. Hu, Y. Liu, D. Zhu, *Chem. Rev.* **2012**, *112*, 2208.
- [21] S. Fratini, M. Nikolka, A. Salleo, G. Schweicher, H. Sirringhaus, *Nat. Mater.* **2020**, *19*, 491.
- [22] Y. Wakayama, R. Hayakawa, K. Higashiguchi, K. Matsuda, *J. Mater. Chem. C* **2020**, *8*, 10956.
- [23] S. H. Yu, S. Z. Hassan, S. Lee, B. Lim, D. S. Chung, *J. Mater. Chem. C* **2023**, *11*, 1560.
- [24] T. Leydecker, M. Herder, E. Pavlica, G. Bratina, S. Hecht, E. Orgiu, P. Samori, *Nat. Nanotechnol.* **2016**, *11*, 769.
- [25] H. N. Tsao, D. Cho, J. W. Andreasen, A. Rouhanipour, D. W. Breiby, W. Pisula, K. Müllen, *Adv. Mater.* **2009**, *21*, 209.
- [26] M. Wang, M. J. Ford, C. Zhou, M. Seifrid, T. Q. Nguyen, G. C. Bazan, *J. Am. Chem. Soc.* **2017**, *139*, 17624.
- [27] Y. H. Lin, W. Huang, P. Pattanasattayavong, J. Lim, R. Li, N. Sakai, J. Panidi, M. J. Hong, C. Ma, N. Wei, N. Wehbe, Z. Fei, M. Heeney, J. G. Labram, T. D. Anthopoulos, H. J. Snaith, *Nat. Commun.* **2019**, *10*, 4475.
- [28] Y. Zheng, G. J. N. Wang, J. Kang, M. Nikolka, H. C. Wu, H. Tran, S. Zhang, H. Yan, H. Chen, P. Y. Yuen, J. Mun, R. H. Dauskardt, I.

- McCulloch, J. B. H. Tok, X. Gu, Z. Bao, *Adv. Funct. Mater.* **2019**, *29*, 1905340.
- [29] M. Nikolka, M. Hurhangee, A. Sadhanala, H. Chen, I. McCulloch, H. Sirringhaus, *Adv. Electron. Mater.* **2018**, *4*, 1700410.
- [30] X. Zhang, H. Bronstein, A. J. Kronemeijer, J. Smith, Y. Kim, R. J. Kline, L. J. Richter, T. D. Anthopoulos, H. Sirringhaus, K. Song, M. Heeney, W. Zhang, I. McCulloch, D. M. DeLongchamp, *Nat. Commun.* **2013**, *4*, 2238.
- [31] W. Zhang, Y. Han, X. Zhu, Z. Fei, Y. Feng, N. D. Treat, H. Faber, N. Stingelin, I. McCulloch, T. D. Anthopoulos, M. Heeney, *Adv. Mater.* **2016**, *28*, 3922.
- [32] Z. Fei, Y. Han, E. Gann, T. Hodsdon, A. S. R. Chesman, C. R. McNeill, T. D. Anthopoulos, M. Heeney, *J. Am. Chem. Soc.* **2017**, *139*, 8552.
- [33] T. Lei, J. H. Dou, J. Pei, *Adv. Mater.* **2012**, *24*, 6457.
- [34] M. El Gemayel, K. Börjesson, M. Herder, D. T. Duong, J. A. Hutchison, C. Ruzié, G. Schweicher, A. Salleo, Y. Geerts, S. Hecht, E. Orgiu, P. Samori, *Nat. Commun.* **2015**, *6*, 6330.
- [35] E. Orgiu, N. Crivillers, M. Herder, L. Grubert, M. Pätzelt, J. Frisch, E. Pavlica, D. T. Duong, G. Bratina, A. Salleo, N. Koch, S. Hecht, P. Samori, *Nat. Chem.* **2012**, *4*, 675.
- [36] I. H. Jung, C. T. Hong, U. H. Lee, Y. H. Kang, K. S. Jang, S. Y. Cho, *Sci. Rep.* **2017**, *7*, 44704.
- [37] M. Herder, F. Eisenreich, A. Bonasera, A. Grafl, L. Grubert, M. Pätzelt, J. Schwarz, S. Hecht, *Chem. - Eur. J.* **2017**, *23*, 3743.
- [38] J. Tian, Z. Liu, W. Jiang, D. Shi, L. Chen, X. Zhang, G. Zhang, C. Di, D. Zhang, *Angew. Chem., Int. Ed.* **2020**, *59*, 13844.
- [39] J. Tian, Z. Liu, C. Wu, W. Jiang, L. Chen, D. Shi, X. Zhang, G. Zhang, D. Zhang, *Adv. Mater.* **2021**, *33*, 2005613.
- [40] S. Schott, U. Chopra, V. Lemaury, A. Melnyk, Y. Olivier, R. Di Pietro, I. Romanov, R. L. Carey, X. Jiao, C. Jellett, M. Little, A. Marks, C. R. McNeill, I. McCulloch, E. R. McNellis, D. Andrienko, D. Beljonne, J. Sinova, H. Sirringhaus, *Nat. Phys.* **2019**, *15*, 814.
- [41] J. Lee, *J. Phys. D: Appl. Phys.* **2021**, *54*, 143002.
- [42] Y. Ie, Y. Okamoto, T. Inoue, T. Seo, T. Ohto, R. Yamada, H. Tada, Y. Aso, *J. Am. Chem. Soc.* **2021**, *143*, 599.
- [43] J. Terao, A. Wadahama, A. Matono, T. Tada, S. Watanabe, S. Seki, T. Fujihara, Y. Tsuji, *Nat. Commun.* **2013**, *4*, 1691.
- [44] H. Qiu, Y. Zhao, Z. Liu, M. Herder, S. Hecht, P. Samori, *Adv. Mater.* **2019**, *31*, 1903402.
- [45] W. Rekab, T. Leydecker, L. Hou, H. Chen, M. Kirkus, C. Cendra, M. Herder, S. Hecht, A. Salleo, I. McCulloch, E. Orgiu, P. Samori, *Adv. Funct. Mater.* **2020**, *30*, 1908944.
- [46] Z. F. Yao, J. Y. Wang, J. Pei, *Chem. Sci.* **2020**, *12*, 1193.
- [47] H. Chen, A. Wadsworth, C. Ma, A. Nanni, W. Zhang, M. Nikolka, A. M. T. Luci, L. M. A. Perdigo, K. J. Thorley, C. Cendra, B. Larson, G. Rumbles, T. D. Anthopoulos, A. Salleo, G. Costantini, H. Sirringhaus, I. McCulloch, *J. Am. Chem. Soc.* **2019**, *141*, 18806.
- [48] T. H. Thomas, D. J. Harkin, A. J. Gillett, V. Lemaury, M. Nikolka, A. Sadhanala, J. M. Richter, J. Armitage, H. Chen, I. McCulloch, S. M. Menke, Y. Olivier, D. Beljonne, H. Sirringhaus, *Nat. Commun.* **2019**, *10*, 2614.
- [49] A. J. Kronemeijer, E. Gili, M. Shahid, J. Rivnay, A. Salleo, M. Heeney, H. Sirringhaus, *Adv. Mater.* **2012**, *24*, 1558.
- [50] Z. Yi, X. Sun, Y. Zhao, Y. Guo, X. Chen, J. Qin, G. Yu, Y. Liu, *Chem. Mater.* **2012**, *24*, 4350.